

Current distortion effects and linear magnetoresistance of inclusions in free-electron metals*

J. B. Sampsell[†] and J. C. Garland

Department of Physics, The Ohio State University, Columbus, Ohio 43210

(Received 16 June 1975)

Exact calculations are given for the magnetic field dependence of the current density near nonconducting spherical and cylindrical inclusions in a free-electron conductor. Some specific results are given in the form of computer-generated drawings of the electric current lines near the inclusions. The magnetoresistance induced by the inclusions is found to be linear in strong magnetic fields with a slope approximately equal to the volume fraction of inclusions. The applicability of the results to the linear magnetoresistance of potassium is discussed.

I. INTRODUCTION

Measurements of transverse magnetoresistance and to a lesser extent, longitudinal magnetoresistance, have provided very useful insights into the galvanomagnetic properties of metals. With regard to gross Fermi-surface structure, the interpretation of measurements is relatively unambiguous; in uncompensated metals the high-field transverse magnetoresistance soars as $(\omega_c\tau)^2$ for open-orbit crystal orientations (ω_c is the cyclotron frequency, τ is the relaxation time), while for closed-orbit orientations it acquires a much weaker field dependence. In recent years there has been a shift of emphasis away from Fermi-surface studies toward more subtle galvanomagnetic effects in metals. Magnetoresistance experiments have been used to study such phenomena as small-angle scattering,¹ magnetic breakdown,² and scattering by strain fields and other lattice imperfections.³ In these studies, which frequently involve the simple metals, the anisotropy of the magnetoresistance is of lesser interest than the field dependence. While no simple description can adequately characterize the results of many experiments, one fact seems clear: The transverse magnetoresistance of pure simple metals seldom, if ever, exhibits the high-field saturation predicted by the theory of Lifshitz, Azbel, and Kaganov.⁴ Instead, the magnetoresistance is usually weakly dependent upon magnetic field, often increasing as a linear function of $\omega_c\tau$. In potassium,^{5,6} for example, the transverse magnetoresistance in strong fields ($\omega_c\tau \gg 1$) obeys the relation $\Delta\rho/\rho(0) = S\omega_c\tau$, where $\Delta\rho = \rho(\omega_c\tau) - \rho(0)$ and where the "Kohler slope" S varies from sample to sample in the range 10^{-4} – 10^{-2} . While there have been a variety of proposed explanations for the linear magnetoresistance of potassium,⁷ the issue is still unresolved and is generally believed to be one of the important unsolved problems in the physics of metals.

It is not at all unusual to find that magnetoresistance measurements of potassium and other simple

metals are not reproducible, but instead vary in a more or less unpredictable way with the details of sample preparation or the precise manner in which voltage and current electrodes are attached.⁶ Furthermore, results are occasionally obtained which are clearly not physically reasonable—for example, a resistance may become negative in strong fields, or a polycrystalline metal may exhibit an anisotropic magnetoresistance.^{6,8,9} Because of the need to isolate the intrinsic properties of a sample from these various spurious effects, there has developed a substantial interest over the past few years in magnetoresistance having geometrical origins and not occurring in a perfectly homogeneous medium. Geometrical magnetoresistance will occur whenever the electric current distribution in a conductor becomes magnetic field dependent, so that the potential difference between voltage electrodes is no longer determined solely by changes in the bulk resistivity of the sample. In principle, current distortions can result from anything which perturbs the potential in an otherwise homogeneous conductor, typical examples being voids, strain fields, lattice defects, surface imperfections, or the existence of voltage and current electrodes. While a redistribution of current lines always increases the total power dissipation in a sample, the current density may be locally reduced or distorted in the vicinity of voltage electrodes. This distortion can lead to an apparent reduction or, in extreme cases, even to a sign reversal of the resistivity. Geometry and electrode magnetoresistance effects of this type have been studied recently Jensen and Smith,¹⁰ Delaney and Pippard,¹¹ and others.^{8,12–15}

The influence of volume inhomogeneities on the galvanomagnetic properties of metals and semiconductors has also received wide theoretical attention. The most common approach has been to derive a statistical expression for the effective conductivity tensor by assuming that inhomogeneities are randomly distributed throughout the medium. Herring,¹⁶ for example, has developed a statistical

model using second-order perturbation theory which is valid for small conductivity fluctuations. An effective medium approach to the problem, which is not restricted to weakly varying conductivities, has been used by Bruggeman,¹⁷ Landauer,¹⁸ Stachowiak,¹⁹ and Stroud.²⁰ A different approach to the problem of bulk volume inhomogeneities is the determination of the current and field profile around a single isolated inhomogeneity such as a void or other discontinuity in the conducting medium. This approach is attractive in that it can provide a physical insight into the problem which is obscured by purely statistical treatments. On the other hand, the boundary-value problem is in general quite complicated for any realistic situation, and the solutions have practical significance only if the medium is so sparsely populated by inclusions that interaction effects are unimportant. Herring¹⁶ has determined the qualitative asymptotic behavior of the current flow at large magnetic fields around an isolated cylindrical inclusion whose axis is parallel to the magnetic field, and has estimated the resultant magnetoresistance to be nearly linear in strong fields. This work has recently been extended by Emets,²¹ who calculated the exact two-dimensional current distribution around an infinitely long cylindrical inclusion having its axis parallel to the magnetic field. Very recently, Ryden²² has obtained the local current density near isolated spherical inclusions for the limiting case of a weak magnetic field. Some general qualitative features of current distortion effects near inclusions have also been discussed by Lass,¹⁴ Delaney and Pippard,¹¹ and Dreizen and Dykhne.²³ In this paper we consider the current distribution and magnetoresistance in free-electron metals induced by voids or other nonconducting inclusions. We are specifically concerned with spherical voids and with cylindrical voids whose axes are transverse to the magnetic field. We believe our results may also be applicable to current distortion effects arising from rough or irregular surfaces. In addition to obtaining the current density, we find that the resulting high-field magnetoresistance is strictly linear with a Kohler slope approximately equal to the volume fraction of voids in the medium. Our calculations are exact and are valid for all values of magnetic field. Because the analytic form of the current-density expressions is quite complex, we have displayed the solutions in the form of computer-generated isometric drawings of the current lines in the vicinity of the inclusions. The explicit expressions are given in the Appendix.

II. PROCEDURE

Our approach is as follows: We consider an infinite homogeneous conducting medium which con-

tains a single nonconducting inclusion. It is assumed that the magnetic field is oriented along the z axis and that the inclusion is located at the origin of the coordinate systems. The medium is described by a free-electron conductivity tensor $\vec{\sigma}$ given by

$$\vec{\sigma} = \sigma_0 \begin{pmatrix} \gamma & \beta\gamma & 0 \\ -\beta\gamma & \gamma & 0 \\ 0 & 0 & 1 \end{pmatrix}, \quad (1)$$

where σ_0 is the zero-field conductivity, $\beta = \omega_c \tau$ is the effective magnetic field, and $\gamma = (1 + \beta^2)^{-1}$. We introduce an electrostatic potential $\Phi(\vec{r})$ which is related to the electric field $\vec{E}(\vec{r})$ and current density $\vec{J}(\vec{r})$ in the usual way: $\vec{E} = -(\nabla\Phi)$ and $\vec{J} = \vec{\sigma}(-\nabla\Phi)$. In a nonzero magnetic field the potential $\Phi(\vec{r})$ does not obey Laplace's equation. However, it is well known¹⁶ that Laplace's equation can be satisfied if a transformation is made to a "scaled" coordinate system defined by $\vec{r}' = \vec{U}\vec{r}$ where \vec{U} is a diagonal matrix given by

$$\vec{U} = \begin{pmatrix} 1 & 0 & 0 \\ 0 & 1 & 0 \\ 0 & 0 & \gamma^{1/2} \end{pmatrix}. \quad (2)$$

Under this coordinate transformation we have $\nabla'^2 \Phi'(\vec{r}') = 0$, and we note that boundaries are compressed along the magnetic field direction by $1/\omega_c \tau$ in strong fields. Thus cylindrical inclusions scale to elliptic cylinders and spherical inclusions become oblate spheroids whose eccentricity increases with magnetic field strength.

The appropriate boundary conditions are that $J_n = 0$ at the surface of the inclusion in the real (unscaled) space and that the current density is uniform at large distances from the inclusion. While in principle these boundary conditions could be used directly by translating the general solution $\Phi'(\vec{r}')$ back into the unscaled coordinate frame to find the specific solution, in practice this procedure becomes extremely complicated. Instead we have found it convenient to introduce a fictitious electric field \vec{E}' given by

$$\vec{E}' = -\nabla'\Phi' = \vec{U}^{-1}\vec{E}. \quad (3)$$

Similarly, we define a scaled current \vec{J}' and conductivity $\vec{\sigma}'$ such that $\vec{J}' = \vec{\sigma}'\vec{E}'$ with

$$\vec{J}' = \gamma^{-1/2}\vec{U}\vec{J} \quad (4)$$

and

$$\vec{\sigma}' = \gamma^{-1/2}\vec{U}\vec{\sigma}\vec{U} = \sigma_0 \gamma^{1/2} \begin{pmatrix} 1 & \beta & 0 \\ -\beta & 1 & 0 \\ 0 & 0 & 1 \end{pmatrix}. \quad (5)$$

It is easily shown that the boundary condition $J_n = 0$ is equivalent to setting $J'_n = 0$, where J'_n is the component of \vec{J}' normal to the scaled inclusion [note

that J'_n cannot be obtained by simply transforming J_n by means of Eq. (4) [inasmuch as angles are not preserved by the transformation]. The electrostatic potential $\Phi'(\vec{r}')$ and the corresponding scaled currents and fields are thus obtained by working entirely within the scaled coordinate system. Once an expression for $\vec{J}'(\vec{r}')$ is found from Eqs. (3) and (5), it is then translated back into the real reference frame using Eq. (4) to obtain the current density \vec{J} . The explicit results of the calculations are given in the Appendix. We remark that our method is not easily applied to the case of conducting inclusions because of the difficulty in matching the normal component of scaled currents at the boundary of the inclusion; the scale transformation \vec{U} would, of course, be different on each side of the boundary.²⁴

III. DISCUSSION

Figure 1 shows the projection on the x - z plane of the electric current distribution [Eqs. (A3)–(A5)] near a cylindrical void for current injected transverse to both the cylinder axis and the magnetic field. At low fields the current distortions disappear about a diameter away from the inclusion. In strong fields, however, the distortions persist for large distances, of order $(\omega_c\tau)R_0$, parallel to the magnetic field. At the same time, the effect of the magnetic field is to shorten or restrict the range of the current distortions for directions transverse to the magnetic field. It is clear from the figure that in the high field limit $\omega_c\tau = \infty$, there

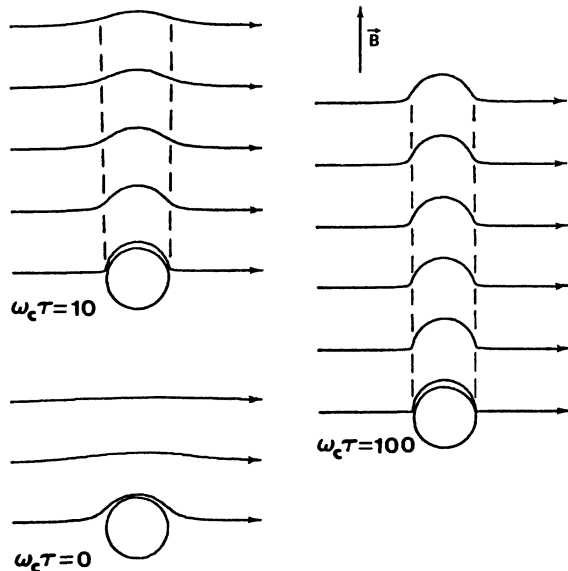


FIG. 1. Projection on the x - z plane of current lines (injected uniformly at $x = +\infty$) in the region near a cylindrical void, for different values of $\omega_c\tau$. The dashed lines indicate regions of high current density.

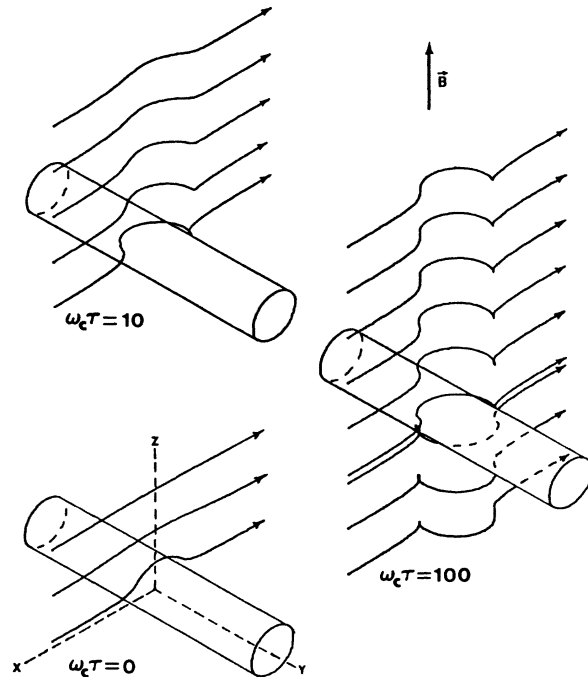


FIG. 2. Isometric projection of the current flow pattern of Fig. 1 illustrating the extent of S-shaped distortions and the high-density current sheets at large $\omega_c\tau$.

are no distortions at all until the current passes through the “shadow” of the inclusion; thus the distortion effects of multiple inclusions may be treated as independent of each other in strong fields so long as the shadows from different inclusions do not intersect. Figure 2 shows a computer-drawn isometric projection of the same current lines illustrating the S-shaped distortion (in the x - y plane) which occurs in strong fields. It should also be noted from Figs. 1 and 2 that as current flows above or below the inclusion it becomes compressed into thin sheets—shown as the dashed lines in Fig. 1—which flow nearly parallel to the magnetic field. The local power dissipation in these sheets may be very great in strong fields and, in fact, it is this dissipation which is primarily responsible for the transverse magnetoresistance induced by the inclusion. This point is illustrated in Fig. 3(a), which shows the variation of the volume power density as a function of x (at a height $z = R_0$ above the inclusion) for different values of $\omega_c\tau$. The curves were obtained by calculating $\vec{J} \cdot \vec{E}$ explicitly from Eqs. (A2)–(A5), and by setting $\vec{J} \cdot \vec{E} = 1$ at large distances from the inclusion. The side lobes evident in Fig. 3(a) at large $\omega_c\tau$ correspond to the Joule dissipation in the vertical current sheets. The transverse magnetoresistance may be obtained by performing a numerical volume integration of the expression for $\vec{J} \cdot \vec{E}$; we have done this and have found that the

magnetoresistance is strictly linear for $\omega_c \tau \geq 10$ with a Kohler slope $S = 1.00f$, where f is the volume fraction of cylindrical voids in the metal.²⁵

Figure 4 shows an isometric drawing of the current flow pattern around a single spherical inclusion for current injected transverse to and parallel to the magnetic field (see Secs. B and C in the Appendix). For the transverse case it is clear that the distortion profile is qualitatively similar to the cylindrical case previously discussed: The distortions are S shaped with the current compressing into a thin shell as it flows above or below the sphere. The high-field transverse magnetoresistance, obtained as before by performing a numerical volume integration of $\vec{J} \cdot \vec{E}$, is also linear with a Kohler slope $S = 0.49f$, where f is the volume fraction of spherical voids.²⁵

For current injected parallel to the magnetic field [see Eqs. (A9)–(A11)], the lines of current above and below the sphere develop a pronounced circulation as shown in Fig. 4. The origins of

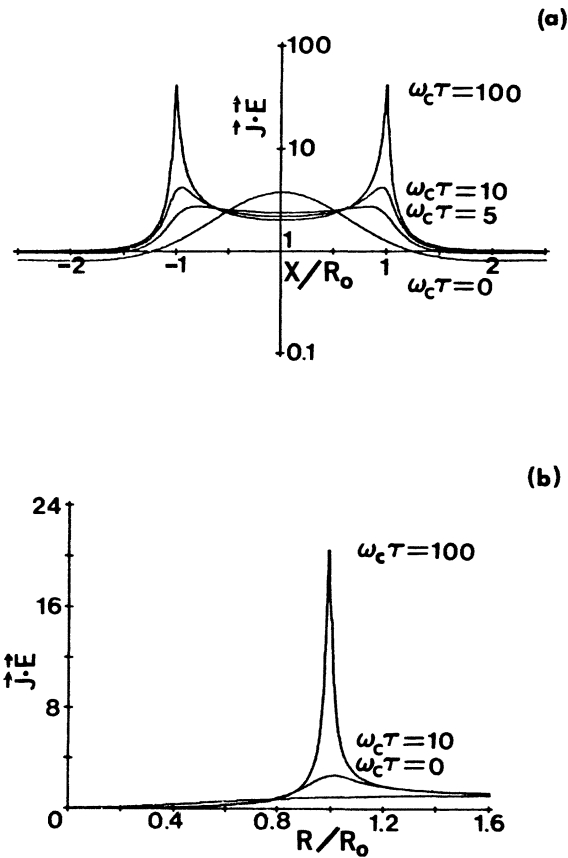


FIG. 3. (a) Volume power density $\vec{J} \cdot \vec{E}$ for the current distribution shown in Figs. 1 and 2 plotted along a line parallel to the x axis which touches the cylinder at $z = R_0$. (b) Radial dependence of the volume power density $\vec{J} \cdot \vec{E}$ for the current distribution shown in Fig. 4(b) plotted in the plane corresponding to $z = R_0$.

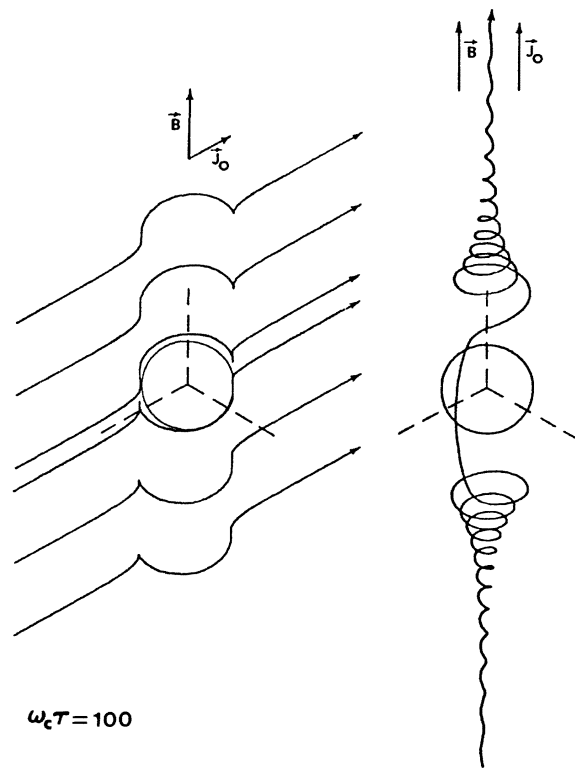


FIG. 4. (a) Isometric projection of current lines (injected uniformly at $x = +\infty$) in the region near a spherical void. (Note $\vec{J}_0 \perp \vec{B}$.) (b) Isometric projection of current lines (injected uniformly at $z = -\infty$) in the region near a spherical void (Note $\vec{J}_0 \parallel \vec{B}$.)

this circulation are the off-diagonal Hall-effect terms in the conductivity tensor which become important where the current begins to sense the perturbing potential of the sphere. Because the conductivity of the medium is very great along the magnetic field direction, the perturbing effect of the sphere persists for large distances, of order $(\omega_c \tau)R_0$, in this direction. It should also be noted that the sense of rotation reverses as the current passes around the equator of the inclusion. The current density within the cylindrical shadow of the inclusion tends to be displaced into a thin shell around the perimeter of the shadow where the power dissipation can be quite large. This is illustrated in Fig. 3(b) which shows the radial dependence of the power density $\vec{J} \cdot \vec{E}$, for several values of magnetic field strength. The curves were obtained from Eqs. (A7)–(A11) at a fixed distance $z = R_0$ above the sphere. The resulting longitudinal magnetoresistance is linear with a Kohler slope $S = 0.64f$ which is about 30% greater than the corresponding transverse magnetoresistance.²⁵

While all of our calculations produce a linear magnetoresistance which scales directly with the

volume fraction of inhomogeneities, we have implicitly assumed that inclusions are so widely separated that interaction effects can be ignored. This is not so stringent a restriction as might be supposed. Because of the inherently one-dimensional character of the distortions, inclusions displaced laterally from one another will never interact. Those inclusions displaced longitudinally will begin to interact only when the magnetic field is sufficiently strong to cause their respective current shells to overlap, i. e., at $\omega_c \tau \geq f^{-1}$. While we cannot anticipate the explicit field dependence resulting from interactions, the narrow width of the current shells suggests that departures from linearity will be small and the onset of interaction effects gradual. For any plausible concentration of voids the magnetoresistance will be linear up to values of $\omega_c \tau$ of several hundred.

While a void concentration $f=10^{-3}$ or smaller may be adequate to account for much of the reported data in potassium or other simple metals, unreasonably large concentrations would be required to explain Kohler slopes of $\sim 10^{-2}$ reported for some specimens. A possible explanation for some of these larger slopes may be obtained by considering the effects of surface roughness or corrosion. That current distortions necessarily accompany an irregular surface may be seen by noting that the solution to the boundary value problem for a spherical void is formally identical to that for current flowing parallel to a flat surface containing a hemispherical indentation (although the resulting magnetoresistance is, of course, only half as large). Furthermore, because a rough surface constitutes, in one sense, a two-dimensional array of laterally displaced indentations, the resulting current distortions are inherently noninteracting until the field is so strong that current shells from opposing faces of the conductor begin to mesh. The linear, surface-induced transverse magnetoresistance has a Kohler slope given approximately by $S = \frac{1}{2}(0.49) \bar{\lambda}/D$, where $\bar{\lambda}$ is a characteristic surface roughness scale factor, and D is the thickness of the specimen measured parallel to the magnetic field. Other types of surface imperfections, such as scratches, can be expected to produce similar effects. Because of the intrinsic dependence on sample size, the linear surface magnetoresistance should exhibit a twofold anisotropy for flat plate samples with the largest resistance occurring when the field is perpendicular to the large face of the plate. In contrast to volume inhomogeneities, surface imperfections produce a saturating longitudinal magnetoresistance.

While our calculations would appear to account for some of the data obtained for potassium and the other simple metals, we wish to stress that no

systematic experimental study of the effects of inclusions on magnetoresistance has yet been reported. Although voids and other inhomogeneities are no doubt present in even the most carefully prepared specimens, it is difficult to obtain a quantitative measure of either their concentration or average size for any given sample. In this regard, we might mention that while our analysis is restricted to the current distortion effects arising from nonconducting macroscopic inclusions, it nevertheless seems reasonable to presume that similar effects will occur whenever there is any spatial fluctuation in the conductivity of the medium. Because of the extremely anisotropic high-field conductivity of free-electron metals, only a slight perturbation of the electrostatic potential, perhaps due to strains or lattice defects, is required to ensure a large distortion of the current pattern. Furthermore, the resulting magnetoresistance will be a linear function of magnetic field because the linearity is a consequence of the anisotropy of the medium and not of the conductivity or geometry of the inhomogeneity.

Finally, we do not believe it is necessary for inhomogeneities to be macroscopic in the conventional sense (comparable to or larger than a mean free path) in order for current distortion effects to be important. Even a small inhomogeneity produces a long range disturbance of the potential which can propagate along the magnetic field for large distances. For example, an inclusion $1 \mu\text{m}$ in diameter will produce a potential distortion about 0.1 mm long at 50 kG in the highest purity potassium now available. On the other hand, our model calculations assume implicitly that the electric field $\vec{E}(\vec{r})$ varies slowly over a distance comparable to a mean free path; while this condition is easily satisfied for electrons moving parallel to the magnetic field, it will be valid for electrons moving in transverse directions only if the inclusions are as large as a mean free path. This does not imply that smaller inclusions necessarily produce smaller current distortions or smaller magnetoresistance. Rather it means that the problem of microscopic inclusions is inherently nonlocal in character and must be approached through more sophisticated techniques than the simple classical approach used here.

The authors are grateful to Professor D. Stroud for helpful discussions.

APPENDIX: ELECTROSTATIC POTENTIALS AND ELECTRIC CURRENT DENSITY NEAR ISOLATED NONCONDUCTING INCLUSIONS

A. Cylindrical inclusion ($\vec{J} \perp \vec{B}$)

Let the conducting medium contain a single infinitely long cylindrical void of radius R_0 whose

axis is aligned along the y axis, and let a uniform current density $\vec{J} = J_{x0} \hat{x}$ be injected at infinity. In the scaled coordinate system it is appropriate to use elliptic cylindrical coordinates (μ, θ, y') given by

$$\begin{aligned} x' &= R_0 \beta \gamma^{1/2} \cosh \mu \cos \theta, \\ z' &= R_0 \beta \gamma^{1/2} \sinh \mu \sin \theta. \end{aligned} \quad (\text{A1})$$

We let μ_0 be the value of μ corresponding to the surface of the inclusion in scaled space and note, from Eq. (A1), that $\sinh \mu_0 = 1/\beta$. Imposing the boundary conditions $J'_\eta = 0$ at $\mu = \mu_0$, and $\vec{J}' = \gamma^{-1/2} \times J_{x0} \hat{x}$ for $\mu \rightarrow \infty$, we find the specific solution to Laplace's equation to be

$$\Phi(\vec{r}') = -(J_{x0}/\sigma_0)(x' + \beta y' + R_0 \gamma^{-1/2} e^{-(\mu - \mu_0)}). \quad (\text{A2})$$

Solving for \vec{J} using Eqs. (4), (5), and (A2) we obtain

$$\begin{aligned} J_x(\mu, \theta) &= J_{x0} \left[1 - \frac{e^{-(\mu - \mu_0)}}{\beta} \right. \\ &\quad \left. \times \left(\frac{\sinh \mu \cos^2 \theta - \cosh \mu \sin^2 \theta}{\sin^2 \theta + \sinh^2 \mu} \right) \right], \end{aligned} \quad (\text{A3})$$

$$J_y(\mu, \theta) = -\beta [J_x(\mu, \theta) - J_{x0}], \quad (\text{A4})$$

$$J_z(\mu, \theta) = -\frac{J_{x0}}{\beta \gamma^{1/2}} e^{\mu_0} \left(\frac{\sin \theta \cos \theta}{\sin^2 \theta + \sinh^2 \mu} \right). \quad (\text{A5})$$

B. Spherical inclusions ($\vec{J} \parallel \vec{B}$)

Let a spherical void of radius R_0 be located at the origin with the magnetic field directed as before. We suppose a uniform current $\vec{J} = J_{x0}$ is injected at infinity parallel to the magnetic field. The appropriate elliptic spheroidal coordinates (η, θ, φ) are

$$\begin{aligned} x' &= R_0 \beta \gamma^{1/2} \cosh \eta \sin \theta \sin \varphi, \\ y' &= R_0 \beta \gamma^{1/2} \cosh \eta \sin \theta \cos \varphi, \\ z' &= R_0 \beta \gamma^{1/2} \sinh \eta \cos \theta, \end{aligned} \quad (\text{A6})$$

and we let η_0 be the value of η corresponding to the boundary of the inclusion in the scaled coordinate system. Imposing boundary conditions, we obtain for the potential $\Phi'(\vec{r}')$ outside the inclusion ($\eta > \eta_0$)

$$\begin{aligned} \Phi'(\vec{r}') &= \frac{J_{x0} \beta R_0}{\sigma_0} \left(\frac{\cosh \eta_0}{[dQ_1(i \sinh \eta)/d\eta]_{\eta_0}} \right. \\ &\quad \left. \times Q_1(i \sinh \eta) - \sinh \eta \right) \cos \theta, \end{aligned} \quad (\text{A7})$$

where $Q_1(z)$ is an associated Legendre function of the second kind, given explicitly by

$$Q_1(z) = \frac{1}{2} z \ln \left(\frac{z+1}{z-1} \right) - 1. \quad (\text{A8})$$

From Eq. (A7) the current density \vec{J} is calculated to be

$$\begin{aligned} J_x(\eta, \theta, \varphi) &= \frac{J_{x0}}{\beta(dQ_1/d\eta)_{\eta_0}} \left(Q_1 \cosh \eta - \frac{dQ_1}{d\eta} \sinh \eta \right) \\ &\quad \times \left(\frac{\cos \theta \sin \theta}{\sinh^2 \eta + \cos^2 \theta} \right) (\cos \varphi + \beta \sin \varphi), \end{aligned} \quad (\text{A9})$$

$$\begin{aligned} J_y(\eta, \theta, \varphi) &= \frac{J_{x0}}{\beta(dQ_1/d\eta)_{\eta_0}} \left(Q_1 \cosh \eta - \frac{dQ_1}{d\eta} \sinh \eta \right) \\ &\quad \times \left(\frac{\cos \theta \sin \theta}{\sinh^2 \eta + \cos^2 \theta} \right) (\sin \varphi - \beta \cos \varphi), \end{aligned} \quad (\text{A10})$$

$$\begin{aligned} J_z(\eta, \theta, \varphi) &= J_{x0} \left[1 - \frac{\cosh \eta_0}{(dQ_1/d\eta)_{\eta_0}} \right. \\ &\quad \left. \times \left(\frac{(dQ_1/d\eta) \cosh \eta \cos^2 \theta + Q_1 \sinh \eta \sin^2 \theta}{\sinh^2 \eta + \cos^2 \theta} \right) \right], \end{aligned} \quad (\text{A11})$$

where the argument of Q_1 is understood to be $i \sinh \eta$.

C. Spherical inclusion ($\vec{J} \perp \vec{B}$)

The explicit solution for the potential for current injection transverse to the magnetic field ($\vec{J} = J_{x0} \hat{x}$ at large distances from the inclusions) is given by

$$\begin{aligned} \Phi(\eta, \theta, \varphi) &= A_1 \cosh \eta \sin \theta (\cos \varphi + \beta \sin \varphi) \\ &\quad + A_2 Q_1^1(i \sinh \eta) \sin \theta \cos \varphi \\ &\quad + A_3 Q_1^1(i \sinh \eta) \sin \theta \sin \varphi, \end{aligned} \quad (\text{A12})$$

where A_1, A_2, A_3 are coefficients having the value

$$A_1 = -J_{x0} R_0 \beta \gamma^{1/2} / \sigma_0, \quad (\text{A13})$$

$$A_2 = \frac{J_{x0} R_0}{\sigma_0 \gamma^{1/2}} \frac{(dQ_1^1/d\eta)_{\eta_0}}{\beta^2 \gamma Q_1^1(i \sinh \eta_0) + (dQ_1^1/d\eta)_{\eta_0}^2}, \quad (\text{A14})$$

$$\begin{aligned} A_3 &= \frac{J_{x0} R_0}{\sigma_0 \gamma \beta Q_1^1(i \sinh \eta_0)} \\ &\quad \times \left(1 - \frac{(dQ_1^1/d\eta)_{\eta_0}^2}{\gamma \beta^2 Q_1^1(i \sinh \eta_0) + (dQ_1^1/d\eta)_{\eta_0}^2} \right). \end{aligned} \quad (\text{A15})$$

In the above expressions the associated Legendre function $Q_1^1(z)$ is related to $Q_1(z)$ by

$$Q_1^1(z) = (z^2 - 1)^{1/2} \frac{dQ_1(z)}{dz}. \quad (\text{A16})$$

The current density $\vec{J}(\vec{r}')$ for this case is obtained exactly as in the preceding examples, but because of the complexity of the expression, will not be given here.

- *Research supported in part by NSF Grant No. GH-33385.
- [†]Ohio State University Graduate Fellow.
- ¹R. L. Powell, in *Proceedings of the Ninth International Conference on Low Temperature Physics*, edited by J. G. Daunt *et al.* (Plenum, New York, 1965), p. 732.
- ²R. J. Balcombe and R. A. Parker, *Philos. Mag.* 21, 533 (1970).
- ³P. A. Penz and R. Bowers, *Phys. Rev.* 172, 991 (1968).
- ⁴I. M. Lifshitz, M. Ya. Azbel, and M. I. Kaganov, *Zh. Eksp. Teor. Fiz.* 31, 63 (1956) [*Sov. Phys. -JETP* 4, 41 (1957)].
- ⁵A summary of recent work may be found in H. Taub, R. L. Schmidt, B. W. Maxfield, and R. Bowers, *Phys. Rev. B* 4, 1134 (1971), and references therein.
- ⁶See J. C. Garland *et al.* *Phys. Rev. B* 9, 1987 (1974), and references therein.
- ⁷Several theoretical models are summarized by L. M. Falicov and H. Smith, *Phys. Rev. Lett.* 29, 124 (1972).
- ⁸W. A. Reed, E. I. Blount, J. A. Marcus, and A. J. Arko, *J. Appl. Phys.* 42, 5453 (1971).
- ⁹J. C. Garland, Ph. D. dissertation (Cornell University, 1969) (unpublished).
- ¹⁰H. H. Jensen and H. Smith, *J. Phys. C* 5, 2867 (1972).
- ¹¹J. A. Delaney and A. B. Pippard, *Rep. Prog. Phys.* 35, 677 (1972).
- ¹²G. DeMey, X. Burvenich, and M. DeMolder, *Phys. Status Solidi A* 23, K45 (1974).
- ¹³G. DeMey, *Solid-State Electron.* 16, 955 (1973).
- ¹⁴J. S. Lass, *J. Phys. C* 3, 1926 (1970).
- ¹⁵M. G. Buehler and G. I. Pearson, *Solid-State Electron.* 9, 395 (1966).
- ¹⁶C. Herring, *J. Appl. Phys.* 31, 1939 (1960).
- ¹⁷D. A. G. Bruggeman, *Ann. Phys. (Leipz.)* 24, 636 (1935).
- ¹⁸R. Landauer, *J. Appl. Phys.* 23, 779 (1952).
- ¹⁹H. Stachowiak, *Physica (Utr.)* 45, 481 (1970).
- ²⁰D. Stroud, *Phys. Rev. B* (to be published).
- ²¹Yu. P. Emets, *Zh. Tekh. Fiz.* 44, 916 (1974) [*Sov. Phys. Tech. Phys.* 19, 586 (1974)].
- ²²D. J. Ryden, *J. Phys. C* 7, 2655 (1974).
- ²³Y. A. Dreizen and A. M. Dykhne, *Zh. Eksp. Teor. Fiz.* 63, 242 (1972) [*Sov. Phys. JETP* 36, 127 (1973)].
- ²⁴It is possible to use this method for conducting spherical inclusions by assuming that the currents and fields within the inclusion are uniform. This has been done implicitly in a study of polycrystalline copper by Stachowiak (see Ref. 19) and by P. M. Martin and J. C. Garland (unpublished).
- ²⁵This result is in agreement with the analytic result of D. Stroud and F. Pan obtained by a Green's-function technique (unpublished).